The EMBO Journal (2004) 23, 739–748 | © 2004 European Molecular Biology Organization | All Rights Reserved 0261-4189/04
www.embojournal.org

THE EMBO JOURNAL

The phagocyte NADPH oxidase depends on cholesterol-enriched membrane microdomains for assembly

Frederik Vilhardt*, Bo van Deurs

Structural Cell Biology Unit, Department of Medical Anatomy, The Panum Institute, Copenhagen, Denmark

The superoxide-producing phagocyte NADPH oxidase consists of a membrane-bound flavocytochrome b_{558} complex, and cytosolic factors p47phox, p67phox and the small GTPase Rac, which translocate to the membrane to assemble the active complex following cell activation. We here show that insolubility of NADPH oxidase subunits in nonionic detergents TX-100, Brij-58, and Brij-98 is a consequence of inclusion into cholesterol-enriched membrane microdomains (lipid rafts). Thus, flavocytochrome b_{558}, in a cholesterol-dependent manner, segregated to the bouyant low-density detergent-resistant membrane (DRM) fraction, and the cytosolic NADPH oxidase factors associated dynamically with low-density DRM. Further, superoxide production following cholesterol depletion was severely compromised in intact cells or in a cell-free reconstituted system, correlating with a reduced translocation of cytosolic phox subunits to the membrane. In analogy with the widely accepted role of lipid rafts as signaling platforms, our data indicate that cholesterol-enriched microdomains act to recruit and/or organize the cytosolic NADPH oxidase factors in the assembly of the active NADPH oxidase.

The EMBO Journal (2004) **23,** 739–748. doi:10.1038/sj.emboj.7600066; Published online 5 February 2004
Subject Categories: membranes & transport; immunology
Keywords: cholesterol; lipid rafts; NADPH oxidase; phagocytes; superoxide

Abbreviations: cyt b_{558}, flavocytochrome b_{558}; CGD, chronic granulomatous disease; DRM, detergent-resistant membrane; l_o and l_d, liquid-ordered and liquid-disordered; mβCD, methyl-β-cyclodextrin; NBT, nitroblue tetrazolium; TnfR, transferrin receptor

Introduction

The superoxide-producing phagocyte NADPH oxidase (NOX-2) plays an instrumental role in host defense. Through the one-electron transfer from NADPH to molecular oxygen, the NADPH oxidase generates superoxide, an important precursor of highly bactericidal reactive oxygen species. When rare mutations of any of the NADPH oxidase subunits render the enzyme nonfunctional, the resulting incapacitation of neutrophils leads to recurrent and life-threatening infections (chronic granulomatous disease; CGD). The NADPH oxidase consists of a membrane-spanning flavocytochrome b_{558} (cyt b_{558}) complex made up of subunits p22phox and the electron-transporting gp91phox. In addition, cytosolic subunits p40phox, p47phox, and p67phox, as well as the small GTPases Rac (1 or 2) and Rap1A are required for enzymatic activity in intact cells, and are recruited to cyt b_{558} in the plasma or phagosomal membrane following cellular activation (Clark *et al*, 1990; Quinn *et al*, 1993). Major fractions of the cytosolic phox proteins p40, p47, and p67phox are thought to exist in a tertiary complex present even under resting conditions (Park *et al*, 1992). Multiple phosphorylations of p47phox unmask epitopes in the complex required for translocation to the membrane, where p47phox and p67phox interact with cyt b_{558} (Park *et al*, 1992; Ago *et al*, 1999). Rac is bound in an inactive cytosolic complex with Rho-GDP dissociation inhibitor, and migrates to the membrane independently of cytosolic phox proteins (Heyworth *et al*, 1994), subsequent to guanine nucleotide exchange (Quinn *et al*, 1993; Bokoch *et al*, 1994). Rac interacts with the membrane through its geranyl lipid modification, and makes direct contacts with p67phox and possibly cyt b_{558} (Bokoch and Diebold, 2002). A continuous translocation of Rac and cytosolic phox proteins to cyt b_{558} in the membrane is required to sustain superoxide production (Dusi *et al*, 1993; Quinn *et al*, 1993), but it is presently unclear which molecular mechanisms lead to termination of NADPH oxidase activity, and how this relates to the acute disassembly of the complex (Dusi *et al*, 1993; DeLeo *et al*, 1999).

In the past, several studies have demonstrated the partial insolubility of neutrophil NADPH oxidase subunits in the nonionic detergent TX-100, a phenomenon that has been attributed to association with the cytoskeleton (Nauseef *et al*, 1991; Woodman *et al*, 1991). However, detergent insolubility may also arise from the segregation of integral or membrane-associated proteins into cholesterol and glycosphingolipid-enriched membrane microdomains termed rafts (Simons and Ikonen, 1997). Indeed, the original and still most widely used criterion of raft association is insolubility in cold nonionic detergents, mainly TX-100 (Brown and Rose, 1992), although alternative detergents such as Lubrol WX and the Brij series have been implemented recently (Madore *et al*, 1999; Roper *et al*, 2000; Chamberlain *et al*, 2001; Drevot *et al*, 2002; Braccia *et al*, 2003). Based on biochemical and biophysical evidence, it is believed that raft lipids form a so-called liquid-ordered phase (l_o), with properties different from those of the liquid-disordered (l_d) phase of surrounding bulk membrane phospholipids. This phase separation critically relies on cholesterol. Current estimates suggest that rafts are small (< 100 nm) and highly dynamic entities (Varma and Mayor, 1998; Pralle *et al*, 2000).

*Corresponding author. Structural Cell Biology Unit, Department of Medical Anatomy, Copenhagen University, Building 18.4, The Panum Institute, Blegdamsvej 3A, 2200 N Copenhagen, Denmark.
Tel: +45 35 32 72 99; Fax: +45 35 32 72 85;
E-mail: f.vilhardt@mai.ku.dk

Received: 4 July 2003; accepted: 12 December 2003; Published online: 5 February 2004

Rafts have been assigned an important role in signal transduction, as they are believed to act as scaffolds for the assemblage of cytosolic factors required for signal propagation from the membrane into the cell (Simons and Toomre, 2000). In the light of the reported partial insolubility of NADPH oxidase subunits in TX-100, ultrastructural evidence of a compartmentalized distribution of NADPH oxidase in the neutrophil plasma membrane (Wientjes *et al*, 1997), and the fact that assembly of the NADPH oxidase holoenzyme requires bringing together a minimum of six different molecular entities (cyt b_{558}, p40, p47, p67phox, Rac1, and Rap1), we hypothesized that NADPH oxidase could be a raft-associated protein. We here show that NADPH oxidase subunits in a cholesterol-dependent fashion are included in low-density detergent-resistant membrane (DRM) indicative of raft localization and, further, that superoxide production is inhibited by cholesterol depletion due to impaired translocation of cytosolic phox protein subunits to the membrane. We propose that lipid rafts function in the recruitment and spatial orientation of cytosolic phox proteins in relation to cyto b_{558}.

Results

cyt b_{558} subunits gp91phox and p22phox segregate to low-density DRM

In intial experiments, we found that a high proportion of gp91phox and p22phox partitioned to the detergent-insoluble pellet in Brij-58 and Brij-98, but not in TX-100 (Supplementary data, Figure 1). To verify that gp91phox and p22phox were genuinely included in a buoyant low-density DRM fraction (indicative of lipid raft localization), we next subjected Brij-58 and Brij-98 detergent extracts from Ra2 and HL60 cells to sucrose density-gradient centrifugation. As seen in Figure 1 A, E, I, and N, a substantial fraction of p22phox and gp91phox floated toward the low-buoyancy top of the gradient, demonstrating association with low-density DRM. A smaller, but significant, fraction of both subunits was contained in the pellet of Ra2 cells (<20% of the total), presumably via association with either detergent-insoluble cytoskeleton or high-density membrane. In Ra2 cells, the transferrin receptor (TnfR), normally thought to be excluded from rafts, was consistently recovered in the first three high-density fractions (⩾90% of the total) regardless of the detergent used (Figure 1C and G). Conversely, flotillin-2 or Lyn, which associate strongly with rafts (Foster *et al*, 2003), floated to low-buoyancy positions in the gradient (Figure 1D, H, M, and Q). Despite the fact that 30–50% of gp91phox resided in high-density fractions 10–12 in Ra2 cells, the vast majority of p22phox co-distributed with gp91phox in low-density fractions. In the case of HL60 cells, flotation of both gp91phox and p22phox was almost quantitative, and codistribution was even more pronounced (Figure 1I and N). Raft proteins acquire detergent insolubility along the biosynthetic route at the stage of transport through the Golgi complex (Brown and Rose, 1992). It is therefore noteworthy that in HL60 cells, the p65-precursor protein of gp91phox, which corresponds to an endoplasmic reticulum intermediate, was completely soluble in Brij detergents, well separated from mature gp91phox at the top of the gradient (see Figure 1I and N). Curiously, a substantial fraction of the TnfR was also present in buoyant low-density DRM in HL60 cells (Figure 1K and O), as has been noted for other cell types

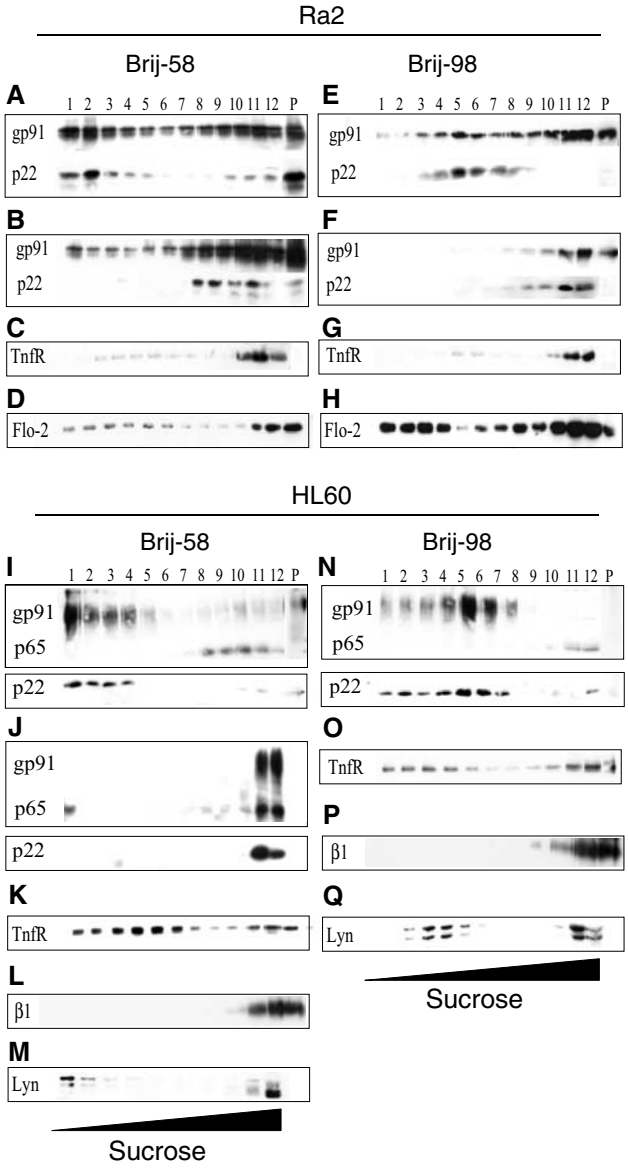

Figure 1 Gp91phox and p22phox segregate to the buoyant low-density detergent (Brij-58, Brij-98) resistant membrane fraction. Ra2 microglia (**A–H**) or HL60 (**I–Q**) cells were lysed in Brij-58 (A–D, I–M) or Brij-98 (E–H, N–Q), in some cases with prior mβCD-facilitated cholesterol extraction (B, F, J), and the lysate was centrifuged to equilibrium in a 35–15% sucrose gradient. Recovered fractions (no. 12 is the bottom, high-density fraction of the gradient) and the solubilized pellet (P) were analyzed by Western blotting using antibodies against gp91phox (gp91), p22phox (p22), transferrin receptor (TfnR), β1-integrin (β1), flotillin-2 (Flo-2), or Lyn as indicated.

(Jutras *et al*, 2003). This phenomenon was also evident when higher concentrations of detergent were used (data not shown). However, the β1-integrin was entirely confined to high-density fractions in HL60 cells, demonstrating differential solubility of membrane proteins in this cell type (Figure 1L and P).

Lipid rafts depend critically on cholesterol, and numerous raft proteins have been shown to redistribute from the detergent-insoluble to the soluble fraction in response to cholesterol depletion (Foster *et al*, 2003). We therefore investigated the effect of cholesterol extraction on cyt b_{558}

distribution, with the aid of methyl-β-cyclodextrin (mβCD), a water-soluble cyclic oligosaccharide with a large capacity for removing cholesterol from cell membranes (Kilsdonk *et al*, 1995). As shown in Figure 1B, F, and J, cholesterol depletion caused the distribution of both gp91phox and p22phox in both cell types to shift markedly toward high-density fractions.

Raft association of cyt b_{558} subunits is predominantly confined to the cell surface

When NADPH oxidase distribution in Ra2 cells was analyzed by immunofluorescence, intracellular gp91phox reactivity was present in addition to plasma membrane staining (Figure 2A–C). In contrast, HL60 cells contain almost all cyt b_{558} reactivity on the plasma membrane (Figure 2D). As the association of cyt b_{558} subunits with low-density DRM was more clear-cut in HL60 cells (compare Figure 1A and E with Figure 1I and N), we examined whether this discrepancy could be explained by the different subcellular distribution of NADPH oxidase in these cells, using a cell surface biotinylation protocol. As seen in Figure 2E and F, surface-resident gp91phox was entirely confined to low-buoyancy positions following extraction in Brij-58 or Brij-98, in contrast to the distribution of total gp91phox in Ra2 cells, which also encompasses the bottom fractions (see Figure 1A and E). Further, while only ca. 10% of the total pool of gp91phox associated with fractions no. 1–8 following TX-100 extraction, this fraction was increased to ∼50% for surface-resident gp91phox (compare Figure 2G with Figure 2H). As before with the Ra2 cells, the TnfR was only present within high-density fractions (Figure 2I). Thus, in Ra2 cells, raft association correlated with cell surface localization of gp91phox.

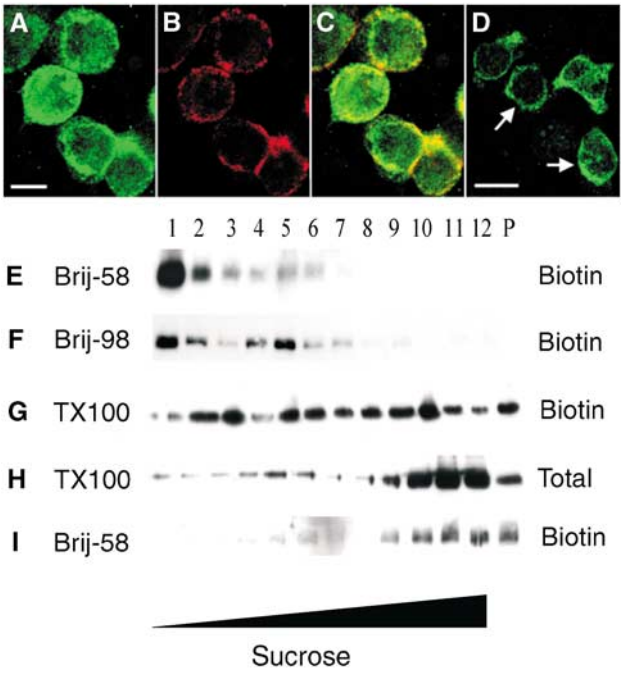

Figure 2 Flavocytochrome b_{558} association with DRM is dependent on the subcellular localization of the complex. (**A–C**) Ra2 cells were incubated on ice with a ricin-HRP conjugate to label the cell surface before fixation. Subsequently, (A) gp91phox was localized with polyclonal anti-gp91phox antibodies, and (B) the cell surface visualized with anti-HRP monoclonal antibody. Panel (C) shows the merged channels, and illustrates that a substantial fraction of gp91phox is present intracellularly. (**D**) For comparison, gp91phox in differentiated HL60 cells is almost exclusively confined to the plasma membrane (arrows). Bars (A–D), 10 μm. (**E–I**) Ra2 cells were surface-biotinylated and extracted in (E, I) Brij-58, (F) Brij-98 or (G, H) TX-100. Subsequent to sucrose gradient centrifugation, biotinylated protein, or in the case of TX-100, also total protein, was analyzed by Western blotting with anti-gp91phox antibodies (E–H) or anti-TnfR antibodies (I).

NADPH oxidase distribution on the plasma membrane is compartmentalized

We sought to establish the raft association of NADPH oxidase by independent techniques. The presumed size of rafts is less than 100 nm (Varma and Mayor, 1998; Pralle *et al*, 2000), falling below the resolution of light microscopical techniques. However antibody-mediated copatching of cell surface antigens has previously been used to demonstrate raft association (Harder *et al*, 1998). Patching of the accepted raft marker ganglioside GM1 with cholera toxin B subunit and antibodies caused gp91phox to copatch with GM1 (Figure 3D–F). In contrast, patching of the TnfR did not lead to any copatching of gp91phox (Figure 3G–I).

We also considered the possibility that a distribution reflecting the raft association of NADPH oxidase could be visualized at the light microscopical level through the use of the enzymatic nitroblue tetrazolium (NBT) test. When NBT is reduced by superoxide, it is converted into a water-insoluble formazan salt, which precipitates as a blue reaction product at the site of superoxide generation. For this purpose, Ra2 microglia were cholesterol-depleted, and the efficiency of cholesterol removal from the plasma membrane was verified by filipin staining (see Figure 4A and B). Subsequently, cells were challenged with PMA in the presence of NBT. As shown in Figure 4C, the reaction product was very clearly not distributed diffusively on the plasma membrane in control cells, but deposited in small patches, indicating that NADPH oxidase distribution on the plasma membrane was compartmentalized. In contrast, if Ra2 cells were cholesterol-extracted with mβCD prior to PMA stimulation, the formazan product was distributed smoothly on the plasma membrane (Figure 4D).

In the control cells, the formazan patches were often seen in association with filopodia- or lammelipodia-like structures (see the inset in Figure 4C). To examine the association of NADPH oxidase activity with the actin cytoskeleton, we performed experiments with the actin-depolymerizing drug latrunculin. As shown in Supplementary Figure 2, latrunculin treatment, followed by drug wash-out, caused the redistribution of NBT patches into large polarized structures on the plasma membrane, which correlated with the formation of dense intracellular foci of F-actin.

NADPH oxidase enzymatic activity requires cholesterol

When performing the NBT test, it became clear that mβCD-extracted cells required a longer time than control cells to develop a visible formazan precipitate. To explore this further, we conducted a series of experiments using the more sensitive luminol-enhanced chemiluminescence technique to measure superoxide release (Wymann *et al*, 1987; Vilhardt *et al*, 2002).

Ra2 cells contain approximately two times as much cholesterol per mg protein than HL60 cells as determined by

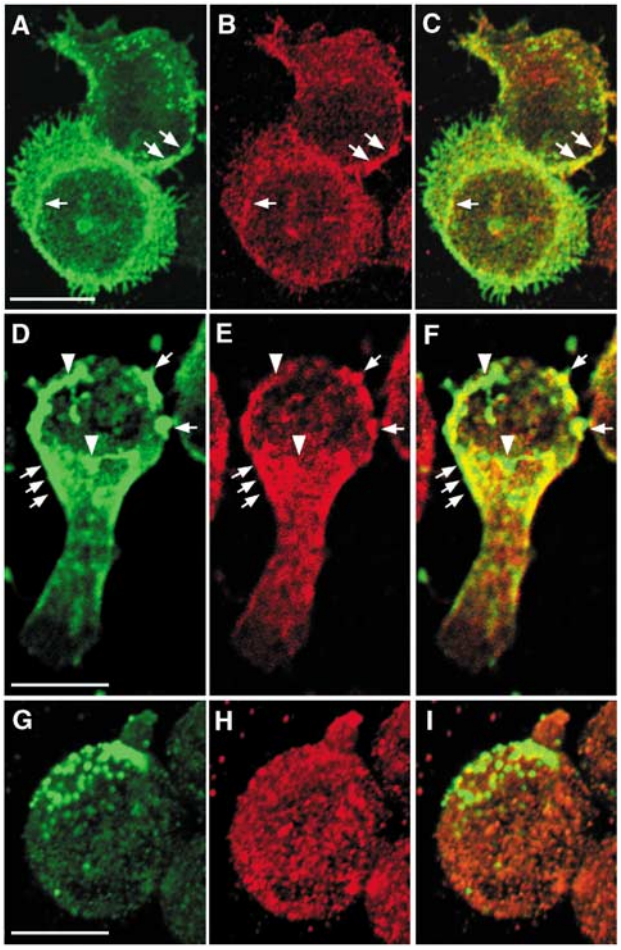

Figure 3 Gp91phox cosegregates with patched ganglioside GM1. GM1 or TnfR on HL60 cells was labeled with Alexa 488-conjugated cholera toxin B subunit (**D–F**) or anti-transferrin receptor antibodies (**G–I**), respectively, and subsequently patched by the addition of secondary antibodies (D–I). Subsequently, immunolocalization of gp91phox (B, E, H) was performed. (**A–C**) shows control cells stained with Alexa 488-conjugated cholera toxin B subunit without secondary antibody patching. Arrows point to areas of colocalization of gp91phox and GM1, while arrowheads denote areas with no apparent overlap. Note the pronounced copatching of gp91phox with GM1 (F), but not transferrin receptor (I). Bars 10 μm.

a cholesterol oxidase/peroxidase-based assay (data not shown), and filipin staining revealed abundant intracellular stores of cholesterol in Ra2 cells (see Figure 4A and B). To deplete Ra2 cells of cholesterol to levels that affected NADPH oxidase activity, it was therefore found essential to culture cells for several days in cholesterol-free serum in the presence of lovastatin (inhibitor of 3-HMG CoA reductase, an early enzyme in the cholesterol synthesis pathway; Brown and Goldstein, 1980) and mevalonate (to rescue isoprenylation of Rac; Bokoch and Prossnitz, 1992), before the final extraction of cholesterol with mβCD. By this method, cellular cholesterol levels were reduced to $61 \pm 8\%$ ($n = 3$) of control cells. Subsequently, superoxide production was determined after stimulation with fMLP, PMA, or IgG-opsonized zymosan particles. As shown in Figure 5A–D, cholesterol extraction caused a dramatic reduction in superoxide production in response to all stimuli. Notably, the greatest inhibition of the oxidative burst was observed for the fMLP-induced response.

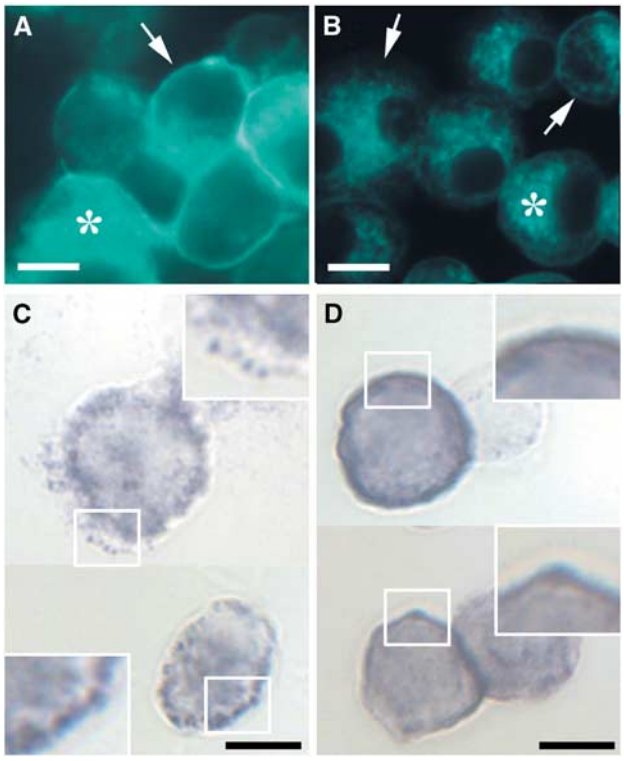

Figure 4 Cholesterol extraction disrupts compartmentalization of NADPH oxidase activity on the plasma membrane. Control (**A, C**) or cholesterol-extracted (**B, D**) Ra2 microglia cells were stained with filipin (A, B) to illustrate the efficiency of cholesterol removal. Asterisks denote intracellular stores of cholesterol (which are partially obscured in (A) due to the intense plasma membrane staining of control cells). Arrows point to plasma membrane staining, which is hardly visible in (B). (**C, D**) Cells were stimulated with PMA in the presence of NBT. Note the pronounced patchy distribution of the precipitation product in the control cells (C), and that cholesterol extraction causes the deposit to become diffusely distributed on the plasma membrane (D). Framed boxes are shown at 2× magnification. Bars (A–D), 10 μm.

HL60 cells contain the majority of both cholesterol and cyt b_{558} in the plasma membrane. As seen in Figure 5E–H, extraction of cholesterol with 10 mM mβCD, which removed $63 \pm 9.8\%$ ($n = 4$) of total cellular cholesterol, was sufficient to inhibit PMA or ionomycin-induced superoxide generation in HL60 cells with 40–60%, and the fMLP-induced response with ca. 95%. Importantly, this deficiency could be overcome if the initial mβCD extraction was followed by incubation with cholesterol-saturated mβCD, which in this case served as a vehicle of cholesterol delivery to the plasma membrane.

Also, filipin, a cholesterol-sequestering agent, inhibited superoxide production by HL60 cells, although the effect was of lower magnitude than that seen for mβCD-mediated cholesterol extraction (Supplementary Figure 3).

Cytosolic NADPH oxidase subunits p67phox and p47phox also associate with low-density DRM, and their membrane translocation is cholesterol-dependent

Cytosolic phox proteins and Rac1 are transported independently to the membrane to associate with cyt b_{558} in response to cell activation (Heyworth *et al*, 1994). When DRM association of p47phox, p67phox, and Rac1 after extraction of HL60 cells in Brij-58 was investigated, we found that small frac-

tions floated to low-buoyancy positions of the gradient (Figure 6A). The DRM association of both phox proteins and Rac1 was evident even under resting conditions, but increased in response to PMA stimulation (Figure 6A). Densiometric quantitation of the Western blots indicated that the relative fraction of p67phox, p47phox, and Rac1 in low-density fractions no. 1–8 increased by a factor of 1.9, 1.2, and 1.1, respectively ($n=2$, variation between experiments $<10\%$). After stimulation the relative fraction of p67phox, p47phox, and Rac1 in low-density DRM constituted 7, 16, and 15% of the total, respectively ($n=2$, variation $<20\%$).

We subsequently analyzed PMA-induced membrane translocation of p47phox, p67phox, and Rac1 in cholesterol-extracted and cholesterol-replenished HL60 cells. Cholesterol extraction severely inhibited translocation (and/or association) of cytosolic phox proteins to the membrane (Figure 6B and D). Rac1 was the least affected by cholesterol removal (percent inhibition of translocation $8\pm25\%$, $n=3$), while p67phox and p47phox were significantly inhibited in their translocation ($63\pm13\%$ and $44\pm4\%$, respectively, $P<0.01$). Importantly, Figure 6C and D shows that when mβCD-extracted cells were replenished with cholesterol before cell stimulation, this translocation deficit was surmounted.

It is known that the association of cytosolic phox proteins and Rac1 with the cyt b_{558} complex is labile. Therefore, considerable fractions of cytosolic subunits are most likely lost from low-density DRM fractions during the long centrifugation step. To demonstrate convincingly that these cytosolic factors are indeed recruited to raft fractions, we used chemical crosslinking with dithiobis-succinimidylpropionate (DTSP) to preserve association with cyt b_{558} (and thereby rafts). As seen in Figure 6E, although the majority of p67phox, p47phox, and Rac1 was associated with high-density membrane, they were also clearly associated with gp91phox and p22phox in low-density DRM.

Efficiency of NADPH oxidase activity in a cell-free reconstituted system depends on cholesterol

Several signaling enzymes important for NADPH oxidase activation are also known to be raft-dependent enzymes. Thus, we found that membrane translocation of PKCβ, known to be important for NADPH oxidase activation in HL60 cells (Korchak *et al*, 1998), was inhibited in cholesterol-extracted cells (Figure 7). Likely, other raft-dependent key players in NADPH oxidase activation, such as phosphoinositide-metabolizing enzymes, could be similarly affected. To decide whether the inhibiting effect of cholesterol depletion on NADPH oxidase activity was indirectly mediated by inhibition of signal transduction, we carried out a series of experiments in a reconstituted cell-free system containing only purified guinea-pig membranes, and recombinant p67phox, p47phox, and GTPγS-loaded Rac1. In this system,

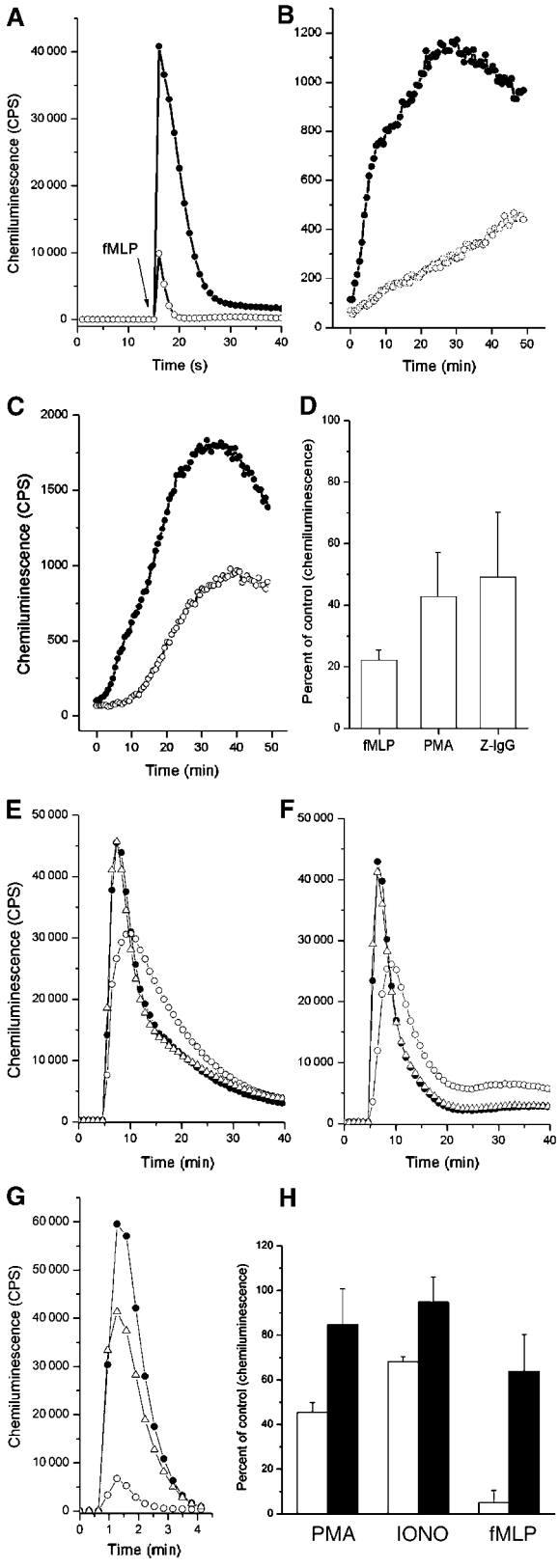

Figure 5 NADPH oxidase activity in Ra2 microglia and HL60 cells requires cholesterol. (**A–D**) Ra2 control (●) or cholesterol-extracted cells (○) were stimulated with (A) fMLP, (B) PMA, or (C) IgG-opsonized zymosan particles, and superoxide production measured continuously by luminol-enhanced chemiluminescence. Bar graph (D) shows mean and s.d. of three independent experiments carried out as in (A–C). Superoxide production of control cells was assigned an arbitrary value of 100. (**E–H**) Control (●), mβCD-extracted (○), or mβCD-extracted and then cholesterol-reconstituted (△) HL60 cells were stimulated with either (E) PMA, (F) ionomycin, or (G) fMLP. Subsequently, superoxide production was measured as above. Bar graph (H) shows mean and s.d. of at least three independent experiments, expressed as percent superoxide production of control cells. Empty bars represent cholesterol-extracted cells, and filled bars represent cholesterol-replenished cells.

membrane translocation of phox proteins is independent of enzymes, and is activated by the addition of anionic amphiphile.

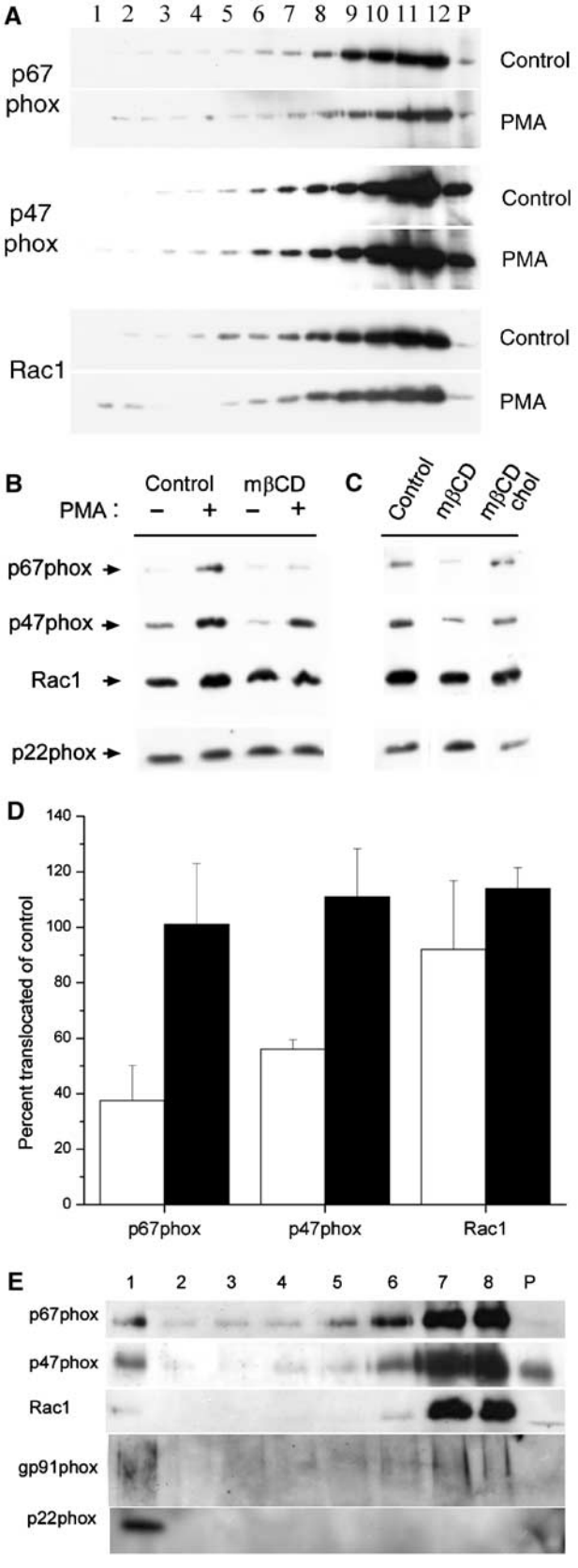

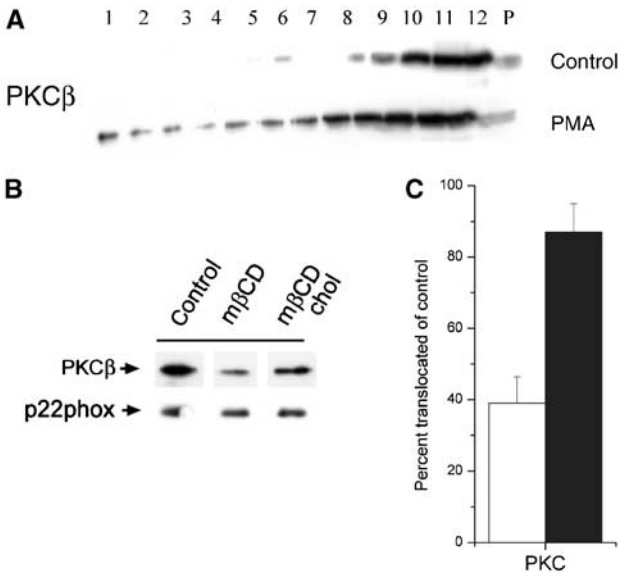

Figure 7 PKC membrane translocation is inhibited after mβCD-mediated cholesterol extraction. (**A**) Brij-58 lysates of control or PMA-stimulated HL60 cells were centrifuged to equilibrium in a sucrose gradient, and then analyzed by Western blotting using antibodies to PKCβ. (**B**) HL60 cells were subjected to cholesterol extraction (mβCD), in some cases followed by cholesterol replenishment (mβCD chol), before stimulation with PMA, and translocation of PKCβ to the particulate membrane fraction analyzed by Western blotting. Equal aliquots were also analyzed for p22phox as loading control. (**C**) The graph represents mean and s.e. of three independent experiments performed as in (B). The results are expressed as percent translocation in cholesterol-extracted (empty bars) or cholesterol-replenished (filled bars) cells relative to control cells.

As seen in Figure 8A, cyt b_{558} in the purified membranes displayed association with low-density DRM similar to that of whole-cell extracts (see Supplementary Figure 1), being mainly soluble in TX-100 and insoluble in Brij-58. When membranes were subjected to mβCD extraction, which removed $75 \pm 6\%$ of membrane cholesterol, a clear solubilization of gp91phox (and p22phox) was apparent. This correlated with a ca. 30% reduction in the rate of superoxide

Figure 6 P47phox and p67phox segregation to low-density detergent (Brij-58) resistant membrane is increased by cell activation, and their membrane translocation is cholesterol-dependent. (**A**) Brij-58 lysates of control or PMA-stimulated HL60 cells were centrifuged to equilibrium in a sucrose gradient, and then analyzed by Western blotting using antibodies to p67phox, p47phox, or Rac1. (**B**) Control or cholesterol-extracted HL60 cells were stimulated with PMA, and subsequently the particulate membrane fraction was analyzed for the presence of p67phox, p47phox, or Rac1 by Western blotting. Equal aliquots were also analyzed for p22phox as loading control. (**C**) HL60 cells were subjected to cholesterol extraction (mβCD), in some cases followed by cholesterol replenishment (mβCD chol), before stimulation with PMA. p67phox, p47phox, Rac1, and p22phox was analyzed by Western blotting as described above. (**D**) The graph represents mean and s.e. of three independent experiments performed as in (C). Individual p67phox, p47phox, and Rac1 bands were quantitated densitometrically, and the results expressed as percent translocation in cholesterol-extracted (white bars) or cholesterol-replenished (filled bars) cells relative to control cells. (**E**) HL60 cells stimulated with PMA were subjected to chemical crosslinking with DTSP and the particulate membrane fraction, purified as above, was subjected to sucrose gradient centrifugation. Collected fractions were electrophoresed under reducing conditions and analyzed by Western blotting with anti-p67phox, p47phox, Rac1, gp91phox, and p22phox antibodies.

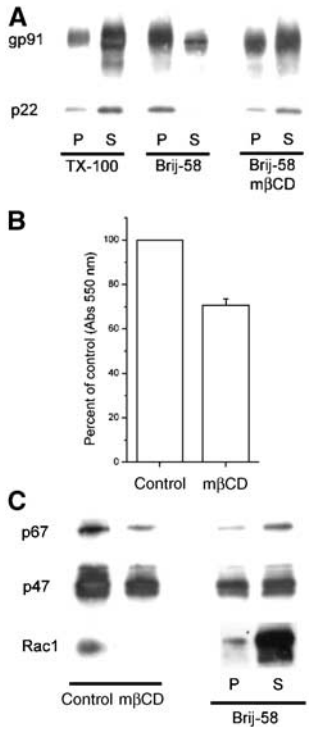

Figure 8 NADPH oxidase assembly and activity in a reconstituted cell-free system depends on cholesterol. (**A**) Control or mβCD-treated purified macrophage membranes were extracted in TX-100 or Brij-58, and distribution of cyt b_{558} subunits in the detergent-insoluble pellet (P) and soluble fraction (S) was determined by Western blotting. (**B**) Superoxide production of control or mβCD-extracted purified macrophage membranes in the reconstituted amphiphile-activated system as measured by cytochrome *c* reduction. Results are expressed as percent cytochrome *c* reduction of control, and represent mean and s.d. of four independent experiments. Superoxide production of control membranes corresponded to 15.9 mol superoxide/mol cyt b_{558} heme/s. (**C**) Control or mβCD-extracted membranes mixed with cytosolic subunits were pelleted, and association of p67phox, p47phox, and Rac1 with membrane determined by lysis in Laemmli buffer and Western blotting. (**D**) Distribution of cytosolic subunits in detergent-insoluble pellet (P) and soluble fraction (S) after extraction of control membranes in Brij-58.

production in the cell-free reconstituted system (Figure 8B), and a reduced recruitment of cytosolic NADPH oxidase subunits to the membrane (Figure 8C), indicating that depression of superoxide generation following cholesterol depletion is in part directly caused by disruption of the raft localization of NADPH oxidase subunits.

Discussion

The present results indicate that the detergent insolubility of NADPH oxidase in Ra2 microglia and HL60 cells relates directly to the localization of NADPH oxidase in cholesterol-enriched membrane microdomains (lipid rafts) for the following reasons: (1) association of cyto b_{558} subunits with low-density DRM was entirely dependent on cholesterol, an important criterion of raft association (Foster *et al*, 2003); (2) cytosolic phox proteins were dynamically recruited to the low-density DRM fraction upon cell activation to attain maximum values of 7–20% of the total, similar to studies in neutrophils where 10–20% of cytosolic phox proteins and Rac translocate to the particulate membrane fraction (Clark *et al*, 1990; Quinn *et al*, 1993; DeLeo *et al*, 1999); (3) membrane translocation of cytosolic phox proteins, and consequently superoxide production, was severely impaired in cholesterol-depleted cells and cell-free membranes; and (4) NADPH oxidase activity on the cell surface was compartmentalized in a cholesterol-dependent manner.

While the role of rafts as signaling platforms in the organization of components in membrane-directed intracellular signaling is by now widely accepted, the phagocyte NADPH oxidase represents one of the first macromolecular enzymatic complexes (not directly involved in cell signaling), which depends on biological rafts for dynamic assembly and enzymatic function (Klopfenstein *et al*, 2002). Many multisubunit proteins, for example, ion channels and membrane receptors, have been identified in low-density DRM or rafts (Foster *et al*, 2003), but in these instances assembly of the holoenzyme is permanent, unlike the situation for the phagocyte NADPH oxidase, which dynamically assembles on rafts in response to external stimuli. In this respect, the NADPH oxidase behaves more akin to the transient assembly of cytosolic signaling complexes on raft microdomains following activation of membrane receptors (Simons and Toomre, 2000).

While this article was under revision, Dekker and coworkers found the efficiency of neutrophil NADPH oxidase activity to depend on lipid rafts (Shao *et al*, 2003). In contrast to our results, mβCD-mediated extraction of cholesterol in neutrophils did not cause a reduction in the magnitude of superoxide release, but rather caused a lag phase before the onset of superoxide production. We believe that this difference is likely caused by the rapid replenishment of plasma membrane cholesterol from intracellular stores, as was sometimes also observed for the Ra2 cells if they were not treated with lovastatin to reduce intracellular cholesterol.

TX100-derived low-density DRM contained low to moderate proportions ($\leqslant$50%) of cyt b_{558} subunits, whereas the segregation of p22phox and gp91phox to low-density fractions was very convincing in the Brij detergents. While the main body of experimental work relating to the study of raft proteins has been performed with TX-100 (Brown and Rose, 1992), the recent recognition of such a differential detergent insolubility of specific proteins has allowed the identification of 'nonclassical' raft proteins, which potentially define novel classes of cholesterol-dependent membrane microdomains (Madore *et al*, 1999; Roper *et al*, 2000; Chamberlain *et al*, 2001; Gomez-Mouton *et al*, 2001; Drevot *et al*, 2002).

In microglia and HL60 cells, raft association was the most important cause of detergent insolubility of NADPH oxidase, and cytoskeletal association accounted for only a minor fraction of the detergent-insoluble pool of NADPH oxidase, based on the small fraction of gp91phox or p22phox ($<$10–20% of the total) recovered in the insoluble pellet after flotation. However, our results are not incompatible with an association of NADPH oxidase subunits with the actin cytoskeleton. On the contrary, as shown in Supplementary data, the NADPH oxidase depends on an intact cytoskeleton, with regard to both superoxide production *per se* and its spatial distribution on the cell surface.

The depression of superoxide production observed in intact Ra2 or HL60 cells is most likely in part the consequence of interference with NADPH oxidase activating enzymes,

such as PKCβ, and probably other raft-dependent regulatory enzymes as well. However, our *in vitro* data from the cell-free reconstituted assay also demonstrate that raft disruption by cholesterol extraction has a direct negative effect on NADPH oxidase assembly and superoxide generation. It is possible that the raft environment presents binding sites for the cytosolic phox proteins, or alternatively the structure of the cyt b_{558} complex is modulated by raft components, to enhance the direct binding of cytosolic subunits with the cyt b_{558} complex. It has been argued that cyt b_{558} plays a major role in the recruitment of cytosolic subunits to the membrane (Heyworth *et al*, 1991; Leusen *et al*, 1994a, b). Nevertheless, Nauseef and co-workers recently showed that cytosolic phox proteins can translocate to, but fail to be retained at, the (phagosomal) membrane in CGD-neutrophils entirely lacking cyt b_{558} subunits (Allen *et al*, 1999), suggesting the presence of other attractors of cytosolic phox proteins in the membrane. Both Rac and cytosolic phoxes are potentially translocated to and/or organized in the plane of the membrane, at least in part, through lipid interactions. Thus, Rac1 requires geranyl modification to support NADPH oxidase activity (Bokoch and Prossnitz, 1992; Vilhardt *et al*, 2002), and recently it has been demonstrated that p40phox and p47phox bind phosphoinositide lipids in the membrane (Kanai *et al*, 2001). Could these lipid-directed interactions take place in a raft environment? While Rac1 in some cell types potentially segregates to DRM (Michaely *et al*, 1999; Kumanogoh *et al*, 2001), prenylated proteins are generally not enriched in rafts (Melkonian *et al*, 1999), and Rac is recruited to the plasma membrane also under conditions of cholesterol depletion, although activation and retainment of Rac1 are compromised (Grimmer *et al*, 2002; Pierini *et al*, 2003). In agreement with this, we found that Rac1 was the the least impaired factor in membrane translocation after cholesterol depletion, likely reflecting that Rac translocates to the membrane by a mechanism independent of rafts but dependent on cyt b_{558} (Heyworth *et al*, 1994). As Rac is a critical component of the NADPH oxidase complex, we have currently no explanation for the apparent lack of a dynamic increase of Rac1 in low-density DRM in intact cells or in the cell-free reconstituted system.

Relatively little is known about the subcellular distribution of phoshoinositide lipids, but some species and phosphoinositide-metabolizing enzymes of relevance to interaction with the phosphoinositide-binding domains of p40phox or p47phox are enriched in rafts (Bodin *et al*, 2001; Galandrini *et al*, 2002). It was, however, recently shown that phosphoinositide interaction is required, but likely not sufficient, for membrane translocation of p47phox (Ago *et al*, 2003). Taken together with the findings of Nauseef and colleagues (Allen *et al*, 1999), the data indicate that assembly of the NADPH oxidase complex depends on multiple weak, but cooperative, binding interactions, presumably greatly favored in a raft environment due to the spatial (pre)concentration of binding partners.

Materials and methods

Cells and materials

The murine microglia cell line Ra2 was cultured in MEM with 10% FCS, 1 ng/ml GM-CSF, and 5 μg/ml insulin, and has been described previously with respect to NADPH oxidase expression and superoxide production (Vilhardt *et al*, 2002), and other phagocyte functions (Inoue *et al*, 1999). The human promyelocytic leukemia cell line HL60 was cultured in RPMI-1640 with 10% FCS, and was differentiated toward the granulocytic lineage by inclusion of 1.3 and 0.65% DMSO in the culture medium for 3 days each. The antibodies used include mouse gp91phox mAb 54.1 (generously donated by Dr Burrit, Department of Microbiology, Montana State University, Bozeman, MT, USA), rabbit gp91phox polyclonal antibody (kindly provided by Dr Francois Morel, Groupe de Recherce et d'Etude du Processus Inflammatoire, University Hospital of Grenoble, France), rabbit p22phox polyclonal antibody (a kind gift from Dr Mary Dinauer, Center for Pediatric Research, Indianapolis, IN, USA), rabbit polyclonal p47phox (a generous gift from Dr William Nauseef, University of Iowa, Iowa City, IA, USA), mouse monoclonal p67phox, Rac1, flotillin-2 and Lyn mAbs (Transduction Laboratories), and mouse transferrin receptor mAbs (Zymed and Ancell). TX100, Brij-58, Brij-98, mβCD, and cholesterol-saturated mβCD were purchased from Sigma.

Detergent solubilization and sucrose gradient centrifugation

Ra2 or HL60 cells were solubilized in 1 ml 1% TX-100, Brij-58 or Brij-98 in 150 mM NaCl, 25 mM Tris—HCl, pH 7.4, with protease-inhibitor cocktail (Boehringer, Mannheim), 10 mM NaF, 10 mM sodium pyrophosphate, and 1 mM sodium vanadate. Loose cell pellets were disrupted with ice-cold TX-100 or Brij-58 by pipetting and left on ice with intermittent whirlimixing for 20 min, while Brij-98 extraction was carried out at 37°C. Detergent extracts were then centrifuged at 4°C in a linear 35–15% sucrose gradient at 155 000 *g* for 17–18 h in a Beckman L8-70M centrifuge. Fractions were collected from the bottom with the aid of a peristaltic pump, and the pellet was solubilized by sonication, for analysis by Western blotting.

We also made use of chemical crosslinking to preserve association of the cytosolic NADPH oxidase subunits with low-density DRM. Briefly, HL60 cells were stimulated at 37°C with PMA in the presence of 1 mg/ml DTSP for the last 60 s. Cells were then rapidly chilled, and crosslinking continued on ice for a further 10 min, before the cells were disrupted by sonication in the presence of 0.3 mg/ml DTSP. Cells were incubated for 15 min on ice before the particulate membrane fraction was purified as described (Leusen *et al*, 1994b), and used for sucrose gradient centrifugation.

To analyze specifically the DRM association of cell surface-localized cyt b_{558}, Ra2 cells in PBS, pH 8.0, were incubated in suspension at 4°C with 0.5 mg/ml *N*-hydroxysulfosuccinimidobiotin (Pierce) for 20 min. Labeling was repeated once, and after quenching of residual biotin, cells were extracted in TX-100, Brij-58, or Brij-98 as above. After sucrose gradient centrifugation, biotinylated protein was precipitated from the collected fractions with streptavidin-conjugated agarose (Sigma) for Western blot analysis of gp91phox.

Alternatively, detergent extracts were fractionated in a bench-top centrifuge (4°C) at 15 000 *g* for 15 min. Subsequently, supernatant (detergent-soluble fraction) and pellet (detergent-insoluble fraction) were recovered and again analyzed by Western blotting.

Immunofluorescense and ganglioside GM-1 patching

Ra2 cells were incubated on ice with 5 μg/ml ricin-HRP (to delineate the cell surface), and washed extensively before fixation. Subsequently, methanol:acetone (50:50 vol:vol) fixed Ra2 and HL60 cells were analyzed, using as primary antibodies rabbit polyclonal anti-gp91phox antibody, and in the case of Ra2 cells, also mouse monoclonal anti-HRP antibody, which were followed by secondary goat-anti mouse Alexa 568 and goat-anti rabbit Alexa 488 antibodies (Molecular Probes) as appropriate. Images were acquired with a Zeiss LSM510 confocal laser scanning microscope with a C-Apochromat ×63, 1.2 water immersion objective, using the argon and helium–neon laser lines for excitation of Alexa 488 and 568, respectively. Sections (1 μm) through medial portions of the cells were collected and saved as 512 × 512-pixel images at 8-bit resolution before import into Adobe Photoshop for compilation.

To visualize raft segregation of gp91phox on a light-microscopical level, we also made use of a cell surface ganglioside GM1 patching procedure. Briefly, HL60 cells were incubated with Alexa 488-conjugated cholera toxin B subunit on ice for 30 min, followed by washing, and a further 30 min incubation with 10 μg/ml mouse monoclonal anti-cholera toxin B subunit. Final patching with 10 μg/ml goat-anti mouse antibodies was carried out for 1 h at 12°C. As a

control, TnfR was patched with monoclonal anti-TnfR antibodies on ice, followed by secondary Alexa 488-conjugated goat-anti mouse antibodies at 12°C. Cells were subsequently fixed in acetone, and immunolocalization of gp91phox was carried out with polyclonal rabbit-anti gp91phox antibodies, followed by Alexa 568-conjugated goat-anti rabbit antibody, as described above.

Cholesterol extraction with mβCD

Ra2 cells seeded at low density were cultured for 3–5 days in MEM with 10% delipidated FCS, 10 μM lovastatin (preactivated by lactone ring cleavage), and 500 μM mevalonate. Cells were then washed and incubated with 20 mM mβCD in Hank's buffered salt solution (HBSS) for 30 min at 37°C with agitation, and washed repeatedly in HBSS to remove traces of mβCD before superoxide measurements or detergent solubilization. DMSO-differentiated HL60 cells were cholesterol-depleted efficiently by mβCD (5–10 mM) extraction alone. In some cases cholesterol extraction was followed by cholesterolreplenishment by incubating cells with 0.5–1 mM cholesterol-saturated mβCD for 30 min at 37°C. The efficiency of cholesterol extraction was verified by measuring cholesterol in detergent-solublized cells using a cholesterol oxidase/peroxidase-based method (Sigma) or, alternatively, visualized by staining with the fluorescent cholesterol-binding drug filipin.

Superoxide measurements

Superoxide production was quantitated using a luminol-enhanced chemiluminescence technique (Wymann *et al*, 1987), essentially as described (Vilhardt *et al*, 2002). Chemiluminescence was measured continuously at 37°C (except for fMLP stimulation of HL60 cells, which was carried out at room temperature) in a Wallac VICTOR microplate reader, before and after stimulation with PMA (100 ng/ml), fMLP (1 μM), ionomycin (250 nM), or IgG-opsonized zymosan, as indicated. To visualize cellular localization of superoxide production, we used NBT. Control or mβCD-extracted Ra2 microglia were incubated in HBSS with 0.25% NBT (Sigma) and 100 ng/ml PMA, and the reaction was allowed to proceed until a satisfactory signal had been obtained before fixation in 2% paraformaldehyde and visual inspection.

Cell-free reconstituted NADPH oxidase system

Purified guinea pig macrophage membranes (Knoller *et al*, 1991) were treated or not with 20 mM mβCD in 100 mM sodium phosphate buffer, pH 7.4, containing 1 mM EGTA, 1 mM $MgCl_2$, 1 mM DTE, 10 μM flavin adenine dinucleotide, 2 mM NaN_3, and 20% glycerol. Membranes were then pelleted at 60 000 *g* for 30 min and resuspended in membrane buffer. Subsequently, superoxide production in the reconstituted cell-free system was performed as described (Toporik *et al*, 1998). Briefly, membrane corresponding to 5 nM cyt b_{558} was mixed with 50 nM of p67phox, p47phox, and GTPγS-loaded Rac1 (generously donated by Prof. E Pick, Tel Aviv University, Israel) in 65 mM sodium–potassium buffer (pH 7.0), 2 mM NaN_3, 1 mM $MgCl_2$, and 10 μM flavin adenine dinucleotide containing 200 μM cytochrome *c* and 130 μM LiDS as an activator. Superoxide production was followed continuously by monitoring superoxide dismutase-inhibitable cytochrome *c* reduction at 550 nm in a Wallac VICTOR microplate reader at room temperature.

Supplementary data

Supplementary data are available at *The EMBO Journal* Online.

Acknowledgements

We thank Izabela Rasmussen, Ulla Hjortenberg, and Mette Ohlsen for expert technical assistance. Dr Michael Danielsen, Department of Biochemistry, Copenhagen University is cordially thanked for help and advice with sucrose gradient centrifugation. We are greatly indebted to Prof. Edgar Pick, The Julius Friedrich Cohnheim-Minerva Center for Phagocyte Research, Tel Aviv University, Israel for his advice and generous gifts of recombinant material for the *in vitro* assays. This work was supported by grants from the Holger Rabitz og hustru Doris Mary, født Philips Foundation, The Desirée and Niels Yde's Foundation, the Danish Medical Research Council (22-02-0551 bmo/mp), the Danish Cancer Society, and The Novo Nordisk Foundation.

References

Ago T, Kuribayashi F, Hiroaki H, Takeya R, Ito T, Kohda D, Sumimoto H (2003) Phosphorylation of p47phox directs phox homology domain from SH3 domain toward phosphoinositides, leading to phagocyte NADPH oxidase activation. *Proc Natl Acad Sci USA* **100:** 4474–4479

Ago T, Nunoi H, Ito T, Sumimoto H (1999) Mechanism for phosphorylation-induced activation of the phagocyte NADPH oxidase protein p47(phox). Triple replacement of serines 303, 304, and 328 with aspartates disrupts the SH3 domain-mediated intramolecular interaction in p47(phox), thereby activating the oxidase. *J Biol Chem* **274:** 33644–33653

Allen LA, DeLeo FR, Gallois A, Toyoshima S, Suzuki K, Nauseef WM (1999) Transient association of the nicotinamide adenine dinucleotide phosphate oxidase subunits p47phox and p67phox with phagosomes in neutrophils from patients with X-linked chronic granulomatous disease. *Blood* **93:** 3521–3530

Bodin S, Giuriato S, Ragab J, Humbel BM, Viala C, Vieu C, Chap H, Payrastre B (2001) Production of phosphatidylinositol 3,4,5-trisphosphate and phosphatidic acid in platelet rafts: evidence for a critical role of cholesterol-enriched domains in human platelet activation. *Biochemistry* **40:** 15290–15299

Bokoch GM, Bohl BP, Chuang TH (1994) Guanine nucleotide exchange regulates membrane translocation of Rac/Rho GTP-binding proteins. *J Biol Chem* **269:** 31674–31679

Bokoch GM, Diebold BA (2002) Current molecular models for NADPH oxidase regulation by Rac GTPase. *Blood* **100:** 2692–2696

Bokoch GM, Prossnitz V (1992) Isoprenoid metabolism is required for stimulation of the respiratory burst oxidase of HL60 cells. *J Clin Invest* **89:** 402–408

Braccia A, Villani M, Immerdal L, Niels-Christiansen LL, Nystrom BT, Hansen GH, Danielsen EM (2003) Microvillar membrane microdomains exist at physiological temperature: Galectin-4's role as lipid raft stabilizer revealed by 'super rafts'. *J Biol Chem* **278:** 15679

Brown DA, Rose JK (1992) Sorting of GPI-anchored proteins to glycolipid-enriched membrane subdomains during transport to the apical cell surface. *Cell* **68:** 533–544

Brown MS, Goldstein JL (1980) Mulitvalent feedback regulation of HMG CoA reductase, a control mechanism coordinating isoprenoid synthesis and cell growth. *J Lipid Res* **21:** 505–517

Chamberlain LH, Burgoyne RD, Gould GW (2001) SNARE proteins are highly enriched in lipid rafts in PC12 cells: implications for the spatial control of exocytosis. *Proc Natl Acad Sci USA* **98:** 5619–5624

Clark RA, Volpp BD, Leidal KG, Nauseef WM (1990) Two cytosolic components of the human neutrophil respiratory burst oxidase translocate to the plasma membrane during cell activation. *J Clin Invest* **85:** 714–721

DeLeo FR, Allen LA, Apicella M, Nauseef WM (1999) NADPH oxidase activation and assembly during phagocytosis. *J Immunol* **163:** 6732–6740

Drevot P, Langlet C, Guo XJ, Bernard AM, Colard O, Chauvin JP, Lasserre R, He HT (2002) TCR signal initiation machinery is preassembled and activated in a subset of membrane rafts. *EMBO J* **21:** 1899–1908

Dusi S, Della Bianca V, Grzeskowiak M, Rossi F (1993) Relationship between phosphorylation and translocation to the plasma membrane of p47phox and p67phox and activation of the NADPH oxidase in normal and Ca(2+)-depleted human neutrophils. *Biochem J* **290:** 173–178

Foster LJ, De Hoog CL, Mann M (2003) Unbiased quantitative proteomics of lipid rafts reveals high specificity for signaling factors. *Proc Natl Acad Sci USA* **100:** 5813–5818

Galandrini R, Tassi I, Mattia G, Lenti L, Piccoli M, Frati L, Santoni A (2002) SH2-containing inositol phosphatase (SHIP-1) transiently translocates to raft domains and modulates CD16-mediated cytotoxicity in human NK cells. *Blood* **100:** 4581–4589

Gomez-Mouton C, Abad JL, Mira E, Lacalle RA, Gallardo E, Jimenez-Baranda S, Illa I, Bernad A, Manes S, Martinez AC (2001) Segregation of leading-edge and uropod components into specific lipid rafts during T cell polarization. *Proc Natl Acad Sci USA* **98:** 9642–9647

Grimmer S, van Deurs B, Sandvig K (2002) Membrane ruffling and macropinocytosis in A431 cells require cholesterol. *J Cell Sci* **115:** 2953–2962

Harder T, Scheiffele P, Verkade P, Simons K (1998) Lipid domain structure of the plasma membrane revealed by patching of membrane components. *J Cell Biol* **141:** 929–942

Heyworth PG, Bohl BP, Bokoch GM, Curnutte JT (1994) Rac translocates independently of the neutrophil NADPH oxidase components p47phox and p67phox. Evidence for its interaction with flavocytochrome b558. *J Biol Chem* **269:** 30749–30752

Heyworth PG, Curnutte JT, Nauseef WM, Volpp BD, Pearson DW, Rosen H, Clark RA (1991) Neutrophil nicotinamide adenine dinucleotide phosphate oxidase assembly. Translocation of p47-phox and p67-phox requires interaction between p47-phox and cytochrome b558. *J Clin Invest* **87:** 352–356

Inoue H, Sawada M, Ryo A, Tanahashi H, Wakatsuki T, Hada A, Kondoh N, Nakagaki K, Takahashi K, Suzumura A, Yamamoto M, Tabira T (1999) Serial analysis of gene expression in a microglial cell line. *Glia* **28:** 265–271

Jutras I, Abrami L, Dautry-Varsat A (2003) Entry of the lymphogranuloma venereum strain of *Chlamydia trachomatis* into host cells involves cholesterol-rich membrane domains. *Infect Immun* **71:** 260–266

Kanai F, Liu H, Field SJ, Akbary H, Matsuo T, Brown GE, Cantley LC, Yaffe MB (2001) The PX domains of p47phox and p40phox bind to lipid products of PI(3)K. *Nat Cell Biol* **3:** 675–678

Kilsdonk EP, Yancey PG, Stoudt GW, Bangerter FW, Johnson WJ, Phillips MC, Rothblat GH (1995) Cellular cholesterol efflux mediated by cyclodextrins. *J Biol Chem* **270:** 17250–17256

Klopfenstein DR, Tomishige M, Stuurman N, Vale RD (2002) Role of phosphatidylinositol(4,5)bisphosphate organization in membrane transport by the Unc104 kinesin motor. *Cell* **109:** 347–358

Knoller S, Shpungin S, Pick E (1991) The membrane-associated component of the amphiphile-activated, cytosol-dependent superoxide-forming NADPH oxidase of macrophages is identical to cytochrome b559. *J Biol Chem* **266:** 2795–2804

Korchak HM, Rossi MW, Kilpatrick LE (1998) Selective role for beta-protein kinase C in signaling for O-2 generation but not degranulation or adherence in differentiated HL60 cells. *J Biol Chem* **273:** 27292–27299

Kumanogoh H, Miyata S, Sokawa Y, Maekawa S (2001) Biochemical and morphological analysis on the localization of Rac1 in neurons. *Neurosci Res* **39:** 189–196

Leusen JH, Bolscher BG, Hilarius PM, Weening RS, Kaulfersch W, Seger RA, Roos D, Verhoeven AJ (1994a) 156Pro–>Gln substitution in the light chain of cytochrome b558 of the human NADPH oxidase (p22-phox) leads to defective translocation of the cytosolic proteins p47-phox and p67-phox. *J Exp Med* **180:** 2329–2334

Leusen JH, de Boer M, Bolscher BG, Hilarius PM, Weening RS, Ochs HD, Roos D, Verhoeven AJ (1994b) A point mutation in gp91-phox of cytochrome b558 of the human NADPH oxidase leading to defective translocation of the cytosolic proteins p47-phox and p67-phox. *J Clin Invest* **93:** 2120–2126

Madore N, Smith KL, Graham CH, Jen A, Brady K, Hall S, Morris R (1999) Functionally different GPI proteins are organized in different domains on the neuronal surface. *EMBO J* **18:** 6917–6926

Melkonian KA, Ostermeyer AG, Chen JZ, Roth MG, Brown DA (1999) Role of lipid modifications in targeting proteins to detergent-resistant membrane rafts. Many raft proteins are acylated, while few are prenylated. *J Biol Chem* **274:** 3910–3917

Michaely PA, Mineo C, Ying YS, Anderson RG (1999) Polarized distribution of endogenous Rac1 and RhoA at the cell surface. *J Biol Chem* **274:** 21430–21436

Nauseef WM, Volpp BD, McCormick S, Leidal KG, Clark RA (1991) Assembly of the neutrophil respiratory burst oxidase. Protein kinase C promotes cytoskeletal and membrane association of cytosolic oxidase components. *J Biol Chem* **266:** 5911–5917

Park JW, Ma M, Ruedi JM, Smith RM, Babior BM (1992) The cytosolic components of the respiratory burst oxidase exist as a M(r) approximately 240,000 complex that acquires a membrane-binding site during activation of the oxidase in a cell-free system. *J Biol Chem* **267:** 17327–17332

Pierini LM, Eddy RJ, Fuortes M, Seveau S, Casulo C, Maxfield FR (2003) Membrane lipid organization is critical for human neutrophil polarization. *J Biol Chem* **278:** 10831–10841

Pralle A, Keller P, Florin EL, Simons K, Horber JK (2000) Sphingolipid-cholesterol rafts diffuse as small entities in the plasma membrane of mammalian cells. *J Cell Biol* **148:** 997–1008

Quinn MT, Evans T, Loetterle LR, Jesaitis AJ, Bokoch GM (1993) Translocation of Rac correlates with NADPH oxidase activation. Evidence for equimolar translocation of oxidase components. *J Biol Chem* **268:** 20983–20987

Roper K, Corbeil D, Huttner WB (2000) Retention of prominin in microvilli reveals distinct cholesterol-based lipid micro-domains in the apical plasma membrane. *Nat Cell Biol* **2:** 582–592

Shao D, Segal AW, Dekker LV (2003) Lipid rafts determine efficiency of NADPH oxidase activation in neutrophils. *FEBS lett* **550:** 101–106

Simons K, Ikonen E (1997) Functional rafts in cell membranes. *Nature* **387:** 569–572

Simons K, Toomre D (2000) Lipid rafts and signal transduction. *Nat Rev Mol Cell Biol* **1:** 31–39

Toporik A, Gorzalczany Y, Hirshberg M, Pick E, Lotan O (1998) Mutational analysis of novel effector domains in Rac1 involved in the activation of nicotinamide adenine dinucleotide phosphate (reduced) oxidase. *Biochemistry* **37:** 7147–7156

Varma R, Mayor S (1998) GPI-anchored proteins are organized in submicron domains at the cell surface. *Nature* **394:** 798–801

Vilhardt F, Plastre O, Sawada M, Suzuki K, Wiznerowicz M, Kiyokawa E, Trono D, Krause K-H (2002) The HIV-1 Nef protein and phagocyte NADPH oxidase activation. *J Biol Chem* **277:** 42136–42143

Wientjes FB, Segal AW, Hartwig JH (1997) Immunoelectron microscopy shows a clustered distribution of NADPH oxidase components in the human neutrophil plasma membrane. *J Leukoc Biol* **61:** 303–312

Woodman RC, Ruedi JM, Jesaitis AJ, Okamura N, Quinn MT, Smith RM, Curnutte JT, Babior BM (1991) Respiratory burst oxidase and three of four oxidase-related polypeptides are associated with the cytoskeleton of human neutrophils. *J Clin Invest* **87:** 1345–1351

Wymann MP, von Tscharner V, Deranleau DA, Baggiolini M (1987) Chemiluminiscence detection of H_2O_2 produced by human neutrophils during the respiratory burst. *Anal Biochem* **165:** 371–378

